KSME

Springer

Journal of Mechanical Science and Technology 37 (4) 2023

Original Article
DOI 10.1007/s12206-023-0319-7

Keywords:
· Bridge cranes
· Dynamics model
· Fatigue life
· Lift impact effect

Correspondence to:
Qisong Qi
qiqisong@tyust.edu.cn

Citation:
Li, C., Qi, Q., Dong, Q., Yu, Y., Fan, Y. (2023). Research on fatigue remaining life of structures for a dynamic lifting process of a bridge crane. Journal of Mechanical Science and Technology 37 (4) (2023) 1789~1801.
http://doi.org/10.1007/s12206-023-0319-7

Received July 7th, 2022
Revised October 11th, 2022
Accepted January 10th, 2023

† Recommended by Editor Chongdu Cho

Research on fatigue remaining life of structures for a dynamic lifting process of a bridge crane

Chenggang Li, Qisong Qi, Qing Dong, Yannan Yu and Yu Fan

College of Mechanical Engineering, Taiyuan University of Science and Technology, Taiyuan 030024, China

Abstract A conventional quasi-static load method causes small stress amplitude and less stress change times when calculating the stress change of crane structures, leading to inaccurate prediction results of the structural fatigue life of the crane. Thus, by investigating the dynamic impact of the crane in the lifting process, the dynamic model of the lifting process was constructed in this study to explore the load variation of a crane structure. A fatigue life prediction method considering the lifting impact effect is proposed to analyze the fatigue life of structures. The calculation results indicate that the lifting impact process increases the number of stress cycles in structures, which has a negative impact on the structural fatigue life. Therefore, determining the dynamic response relationship between the lifting impact effect and the fatigue life of a crane structure can help improve the safety of this structure.

1. Introduction

In recent years, cranes have been widely used as basic equipment of the national economy. Considering the structural fatigue problem caused by the poor service environment of cranes, worldwide scholars that focus on machinery-related topics have carried out many structural fatigue life predictions [1, 2] and design work based on fatigue strength [3-5]. Wang [6] of Aircraft Strength Research Institute of China proposed key issues to be considered and investigated in a longer period: the fatigue damage response relationship of structures under the influence of multiple engineering environments and experiments of multi-physical field coupled loading fatigue. On this basis, fatigue and optimization designs of vibration and impact resistance should be the focus of future structural designs. As special equipment, the main form of damage to the crane's structure is also fatigue, and its service life will be frequently subjected to structural vibration and other load effects. Therefore, research on the fatigue strength decay mechanism under the influence of multiple factors for crane structures is significant for crane safety.

Currently, the crane structure fatigue strength and life prediction and other technical topics have become a hot spot in academia. The difficulty of the problem is mainly reflected in the mechanism of the crane structure fatigue strength impact, investigations of the remaining life prediction, the dynamic load effect of special working conditions, etc. Consequently, many studies have been conducted by researchers from China and other countries. For example, Wang et al. [7] conducted a numerical study on the fatigue life prediction of an aircraft tail structure under the action of multi-point coordinated load spectrum. Shin et al. [8] derived and determined a load spectrum model for this type of crane by examining the measured load data of multiple offshore cranes in service. Dong et al. [9] predicted two-parameter stress spectra of casting cranes using the rain-flow counting method. Wang et al. [10] used likelihood ratio detection and Latin hypercube sampling to capture the optimal parametric probability distribution model of the load-stress history, thereby obtaining the stress spectrum required for life prediction. Nejad et al. [11] investigated the effect of spectral load ing on the fatigue life and crack propagation of structures. Chen et al. [12] explored the vibration characteristics of wheel-rail friction system by establishing a crane wheel-rail coupling dynamics model, which is based on an Abaqus implicit dynamics algorithm. Martins et al. [13] used known aircraft load spectra to predict and analyze the fatigue life of aircraft structures by using Abaqus (C) finite element and extended finite element methods. Qu et al. [14] established a damage degradation model of steel structures, judged the damage accumulation for the stress state of each dangerous point of the bridge crane, and then assessed the early life of the crane structure. Lu et al. [15] analyzed the typical working conditions of tower cranes and used ANSYS combined with ADAMS for rigid-flexible coupling dynamics simulation to obtain the load spectrum under the working cycle. Liu et al. [16] used the FE-SAFE fatigue analysis software to investigate the fatigue life of the tower arm welded joints. Yang et al. [17] examined the fatigue life of a crane girder under the impact caused by different track height differences by developing a virtual prototype for motion simulation. Wei et al. [18] proposed a moving load treatment method with pulse load superposition; they obtained the overall fatigue life field of the main girder structure based on the equivalent structural stress method. Ávila et al. [19] investigated the combination of S-N and finite element method for fatigue life prediction of cranes. Euler et al. [20] proposed a fatigue load prediction method for runway beams based on the type of crane operations. Rettenmeier et al. [21] evaluated the effect of multi-axial stress states caused by crane wheel loads and welding residual stresses on the life of a crane runway girder. Li et al. [22] simulated the instantaneous effect of sudden unloading for two working conditions of truck cranes; they obtained the change of boom under the corresponding working conditions. Xin et al. [23] analyzed the influence of operating speed and rail defects on the crane impact coefficient; they also analyzed the influence of rail defects on crane crack propagation and fatigue life.

These studies have attempted to predict the fatigue remaining life of mechanical products. However, no in-depth investigation has been conducted on the influence of the dynamic effects of mechanical products under complex operating conditions on the fatigue bearing capacity of structures. Therefore, this paper proposes to consider the load variation caused by structural vibration in the process of analyzing the fatigue life of crane structures. The research object is the lifting process in crane operation, aiming at the structural vibration caused by the lifting process of a cargo. Further, the influence of dynamic lifting effect on the fatigue strength and fatigue remaining life of the structure is analyzed by developing a dynamics model. The study significant for the fatigue strength design of crane structures and crane safety in service.

2. Dynamic characteristics of the crane lifting process

Each workflow of a crane requires a load lifting operation. Frequent lifting and unloading of materials trigger fluctuations in the load and stress indicators of the crane structure and may lead to the continuous accumulation of internal defects or damage to the structure, eventually resulting in fatigue damage. Moreover, the structural vibration phenomenon that happens during load lifting of the crane always occurs and is inevitable. This structural vibration increases the stress amplitude of the crane structure and the number of stress cycles and hence negatively impacts the structure life. Therefore, for the dynamics modeling of the crane lifting process, the rigid-flexible coupling characteristics of the crane structure, mechanism, and components during the load lifting process should be fully considered. In this study, the influence of load lifting on the load characteristics and stress indicators of the crane structure is clarified by constructing a dynamics model of the lifting process.

2.1 Dynamics model of the lifting process

An appropriate dynamics model of load lifting is crucial for investigating the dynamic load effect of the crane lifting process. Table 1 presents a typical process for crane load lifting. As shown in the four lifting stages of the tables, the reason for the dynamic effect of the load lifting process on the crane structure

Table 1. Load lifting process.

The first stage	The second stage	The third stage	The fourth stage
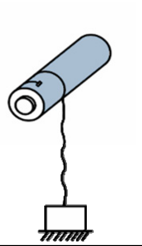	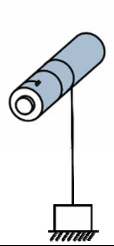	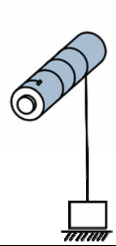	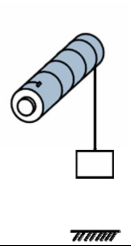
Cargo rests on the ground and the wire rope is slack and not under stress	The cargo is at rest and the wire rope starts to be gradually stretched to $F = mg$	The cargo leaves the ground. Wire rope tension suddenly increased to $F = \varphi mg$ and the impact on the structure	The cargo is lifted through the process of acceleration, uniformity, and deceleration to reach the specified height

Table 2. Definitions of the symbols of the hoisting mechanism dynamics model presented in Fig. 1.

Symbols	Physical meaning	Unit	Symbols	Physical meaning	Unit
m_1	Self-weight of bridge structure	kg	c_0	Damping coefficients of elastic couplings and reducer-related components	(N·s)/m
c_1	Damping factor of bridge structure	(N·s)/m	c_2	Damping coefficient of steel wire rope of pulley set	(N·s)/m
k_1	Bridge structural stiffness	N/m	k_0	Stiffness of elastic couplings and reducer-related components	N/m
m_2	Pick-up device and cargo quality	kg	θ_1	Angular displacement of J_1	rad
k_2	Damping coefficient of steel wire rope of pulley set	N/m	θ_2	Angular displacement of J_2	rad
J_1	Equivalent rotational inertia of motor and flexible coupling part	kg·m^2	x_1	Bridge displacement	m
J_2	Equivalent rotational inertia of transmission parts such as brakes and reducers	kg·m^2	x_2	Hook displacement, i.e. item displacement	m

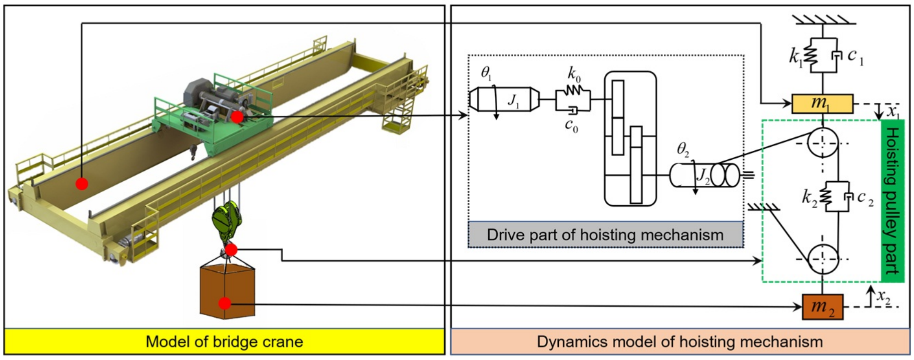

Fig. 1. Dynamics model of the bridge crane hoisting mechanism.

is because, when the cargo is lifted off the ground without restraint, the dynamic effect of the sudden increase in lifting load will occur due to inertia force. Consequently, the dynamic load impact on the crane structure causes structural vibration.

Based on the composition characteristics of the whole bridge crane and the dynamic characteristics of the load lifting process, the dynamics model of the crane lifting process (Fig. 1) is established using the dynamics theory. The components of the crane's hoisting mechanism are divided into driving and driven parts. The driving part includes the driving motor, elastic coupling, reducer, and reel, whereas the driven part includes the pulley set, wire rope, hook, and load. To accurately and effectively simulate the transmission process of the hoisting mechanism using the dynamics model, as well as better restore the working condition of the hoisting mechanism. The vibration damping function of the flexible coupling was retained in the process of simplifying the dynamics modeling of the hoisting mechanism. Simultaneously, the wire rope is simplified to an elastomer with the same stiffness and damping parameters. As the dynamic effects presented by the crane structure during load lifting are mainly reflected in the main girder, the crane main girder is simplified to concentrate loading and retain its vibration characteristics. Fig. 1 shows the simplified dynamics model of the crane lifting process, which has the dynamics of 4-degrees-of freedom and four masses. Table 2 presents the definition of the symbols in Fig. 1.

According to the lifting process dynamics model, the force of each mass unit is analyzed using Newton's second law, and the dynamics equation is derived, as expressed in Eq. (1).

$$\begin{cases} \begin{pmatrix} J_1 & J_2 \end{pmatrix}\begin{pmatrix} \ddot{\theta}_1 \\ \ddot{\theta}_2 \end{pmatrix} + c_0\begin{pmatrix} \dot{\theta}_1 - \dot{\theta}_2 \\ \dot{\theta}_2 - \dot{\theta}_1 \end{pmatrix} + k_0\begin{pmatrix} \theta_1 - \theta_2 \\ \theta_2 - \theta_1 \end{pmatrix} = \begin{pmatrix} M_T \\ -\dfrac{FR}{i} \end{pmatrix} \\ \begin{pmatrix} m_1 & m_2 \end{pmatrix}\begin{pmatrix} \ddot{x}_1 \\ \ddot{x}_2 \end{pmatrix} + c_1\begin{pmatrix} \dot{x}_1 \\ 0 \end{pmatrix} + \begin{pmatrix} k_1 & k_2 \end{pmatrix}\begin{pmatrix} x_1 \\ x_2 \end{pmatrix} = \begin{pmatrix} nF + m_1 g \\ nF - m_2 g \end{pmatrix} \\ F = k_2\left(\dfrac{R\theta_2}{in} - x_1 - x_2\right) + c_2\left(\dfrac{R\dot{\theta}_2}{in} - \dot{x}_1 - \dot{x}_2\right) + \dfrac{m_2 g}{n} \end{cases} \quad (1)$$

where M_T denotes the output torque of the motor; F, wire rope traction force; R, radius of the reel; n, pulley set multiplier; and i, total transmission ratio.

2.2 Coefficients of the dynamics model

The dynamics model of the crane lifting process has three main components: mass (rotational inertia), damping, and stiffness. Regarding the transient impact on the structure, damping allows the system to recover to a steady state, whereas stiffness characterizes the ease of elastic deformation of the structure. Thus, in a study on the dynamic load effect of a crane, a reasonable transformation of the parameters of each part of the crane is key to simulate the vibration characteristics and elasticity effect of the actual system. Meanwhile, the parameters required for the model are determined based on the principle of conservation of work and energy so that the actual crane system can be converted to an equivalent model system.

1) Rotational inertia of the hoisting mechanism

Due to the rotational operating feature of the drive motor of the hoisting mechanism, the masses of the driving and driven parts are converted into the equivalent rotational inertia. According to the kinetic energy theorem and the law of conservation of energy, when a moving part in a moving component transfers its mass to a specified part, the equivalent rotational inertia of the specified part can be expressed by Eq. (2).

$$J_L = \sum_{k=1}^{M} J_k \left(\frac{\omega_k}{\omega}\right)^2 + \sum_{j=1}^{N} m_j \left(\frac{v_j}{\omega}\right)^2 = \sum_{k=1}^{M} \frac{J_k}{i_j^2} + \sum_{j=1}^{N} \frac{m_j}{i_j^2} \tag{2}$$

where J_k denotes the $k\text{-}th$ rotating parts; ω_k, angular velocity of the $k\text{-}th$ parts; m_j, $j\text{-}th$ moving parts; and v_j, speed of the $j\text{-}th$ moving parts.

2) Equivalent mass of the crane main girder

In the process of developing the dynamics model of crane lifting conditions, due to the large span of the main girder and its deformation under load, the mechanical properties of this girder must be considered when converting the equivalent mass of this girder. The main girder is subjected to both self-weight and vertical concentrated loads during service. As the upper arch is preset in the design, only the deformation due to concentrated loading is considered in the equivalent calculation of the main girder's mass. Given the general features of the bridge crane structure, when the span of the main girder is subjected to concentrated load, the mid-span section of the main girder has the maximum deflection. The structure of the crane's main girder can be simplified to a simply supported beam (Fig. 2). Combined with the influence line of deflection of a simply supported beam under load, the dynamic deflection characteristics of the main girder under concentrated load in the mid-span of the main girder can be derived, as expressed in Eq. (3).

$$\begin{cases} y(x,t) = y_c(t) f(x) \\ f(x) = 3\left(\frac{x}{l}\right) - 4\left(\frac{x}{l}\right)^3 \\ 0 \le x \le l/2 \end{cases} \tag{3}$$

where x represents the distance from the deformation point to the left endpoint. When the concentrated load borne by the crane's structural layer is located at the mid-span of the main girder, the deformation on both sides of the mid-span section of the crane is consistent. Hence, the value range of x is set to half of the span l; y_c is the mid-point deflection of the main girder, which is a function $y_c = y_c(t)$ at the time when the main beam structure vibrates; and $f(x)$ is the shape function of the beam vibration.

From the shape function $f(x)$ in Eq. (3), the deflection at a point of a simply supported beam during vibration is only related to the location of that point. Thus, the angular velocity at each point on the main girder can be derived using Eq. (4). Let the mass of the girder per unit length be ρ. Eq. (5) is used to calculate both the kinetic energy and the equivalent mass of the main girder. Thus, taking $x = l/2$ under the premise of retaining the mechanical properties and vibration characteristics of the main beam, the calculation according to Eq. (6) can be obtained by taking 17/35 of the total mass of the main girder as the equivalent mass of the main girder in the dynamic model.

$$\frac{\partial y(x,t)}{\partial t} = \dot{y}_c(t) f(x) \tag{4}$$

$$T = 2\int_0^{\frac{l}{2}} \frac{1}{2}\rho\left[\frac{\partial y(x,t)}{\partial t}\right]^2 ds = \frac{1}{2}\rho \dot{y}_c^2(t)\int_0^{\frac{1}{2}} f^2(x)dx = \frac{1}{2} m_e \dot{y}_c^2(t) \tag{5}$$

$$m_e = 2\rho\int_0^{\frac{1}{2}}\left[3\left(\frac{x}{l}\right) - 4\left(\frac{x}{l}\right)^3\right]^2 dx = \frac{17}{35}\rho l = \frac{17}{35} m' \tag{6}$$

where $\dot{y}_c(t)$ is the first-order derivative of the deflection at the mid-point of the main girder, m_e is the equivalent mass of the main girder, and m' is the actual mass of the main girder.

3) Equivalent stiffness and equivalent damping

Under the same load condition, the degree of deformation of the simply supported beam is determined by the stiffness, and the stiffness and deformation size have an inverse ratio property. The main girder, as the main load-bearing member of the crane, determines its stiffness in terms of section form, span, and materials. Based on this, the crane's main girder stiffness is calculated using Eq. (7).

The deformation of a wire rope, as the direct force member of cargo hoisting, also affects the impact of load changes on the structure. In actual work, the stiffness of a wire rope and the rope length are inversely proportional. Thus, in the process of winding a wire rope, its stiffness will also change accordingly. However, the lifting height of the crane is often less than 20 m,

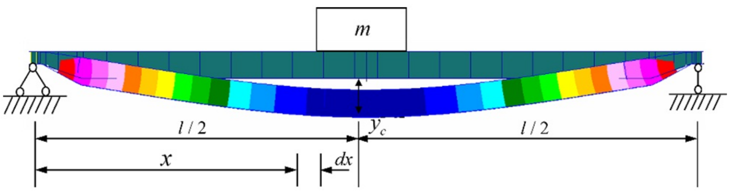

Fig. 2. Simplified diagram of the bridge structure.

and hoisting mechanism running time is short. Further, the effect of the lifting process on the wire rope deformation is small; thus, the wire rope stiffness is assumed to be constant. The stiffness of a single wire rope can be calculated using Eq. (8).

In the process of lifting the cargo off the ground, the structure will be impacted and forced to vibrate. This structure vibration is gradually attenuated and eventually stabilized by the damping effect of the system. Based on the principle of equal energy dissipation, the energy dissipated through equivalent viscous damping is equal to that dissipated by the actual damping within a vibration cycle. Specifically, the equivalent viscous damping method is used to calculate the crane's main girder and wire rope damping, as expressed in Eq. (9).

$$k_1 = \frac{48EI}{L^3} \quad (7)$$

$$k_s = E_r A / l \quad (8)$$

$$c_{eq} = 2m\omega_n \xi_{eq} \quad (9)$$

where E is the modulus of elasticity of the main girder, I is the moment of inertia of the main girder section, L is the span of the main girder, E_r is the elasticity coefficient of the wire rope, A is the cross-sectional area of the wire rope, l is the length of the wire rope, m is the corresponding object mass, ω_n is the natural frequency of the system, and ξ_{eq} is the equivalent damping ratio.

3. Calculation method of the crane fatigue life based on fracture mechanics

Crane fatigue life is the number of stress or strain cycles required to generate fatigue damage in a structure. Therefore, the change in structural stress under operating conditions should be obtained to predict fatigue life. Based on the fatigue life calculation method of fracture mechanics, the above dynamics model is used to obtain the dynamic load change during the lifting process and then obtain the stress-time history of the entire working cycle. Finally, the fatigue life of the crane structure can be predicted.

3.1 Crane fatigue life analysis

Under normal service conditions, the damage to the crane's metal structure often undergoes the following three stages: crack sprouting, stable crack expansion, and overall structural damage. Crack sprouting is the basic factor that causes structural damage. Due to the possibility of potential initial defects in manufacturing, welding, and even steel rolling process, the crane structure under long-term heavy load and high-frequency service conditions undergoes a defect expansion phenomenon. When structural defects (e.g., cracks) extend to a certain size, this results in the failure of the crane structure, possibly leading to critical accidents. In the above process of structural defects (cracks), the expansion process is caused by the superposition of multiple loads during the service period. Data-driven quantification and calculation methods between load characteristics in service and crack expansion patterns are available. Therefore, accurate evaluation of the fatigue crack expansion mode of crane structures and calculating the crack expansion process are key to predict the crane's fatigue life. Fig. 3 presents the general process of fatigue life calculation. The figure also shows that the primary task of fatigue remaining life calculation of structures is to determine the stress-time history of a structure's critical parts under specific operating conditions. The above dynamics model can be applied to obtain the stress variation in the structure during the lifting impact throughout the work cycle. Subsequently, the load history is analyzed and processed using the structural mechanics theory and a rain-flow counting method, and the stress variation characteristics and trend at test points are obtained. Finally, analysis of the fatigue crack extension of the structure is combined with the Paris formula and fracture mechanics theory to calculate and determine the fatigue remaining life value of the crane structure.

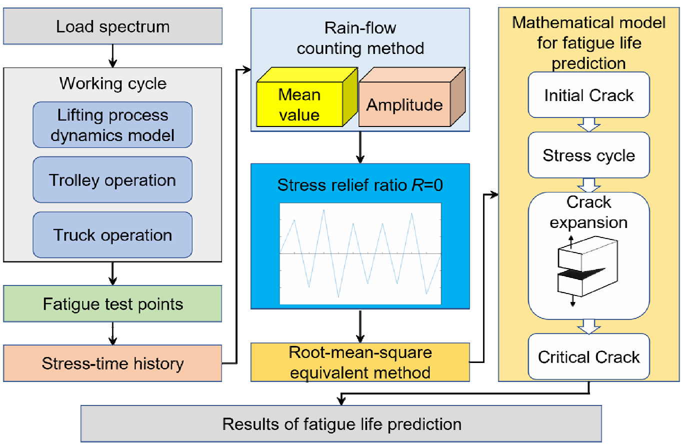

Fig. 3. Flow chart of the fatigue life calculation.

3.2 Stress-time history acquisition

The crane's structure in a service motion state is typically subjected to a variety of dynamic loads acting together. By analyzing the mechanical model of the main girder, the stress levels are calculated at the test points at the dangerous sections of the structure under the action of each internal force. Thus, the most unfavorable stress-time histories are obtained, and the basis for predicting the fatigue life of the structure is determine.

1) Stress calculation models

The main girder is subjected to uniform and concentrated loads during crane service. In this process, the trolley reciprocates on the main girder to form a moving load, and the stress levels in each section of the main girder change accordingly. The bridge structure mechanics model is presented in Fig. 4, and the physical meaning of each symbol in the figure is provided in Table 3. Lifting trolley straddles two main girders. As shown in Fig. 4, the red arrows in the vertical direction (i.e., Y-axis) represent the position of the trolley wheel pressure, and the black uniformly distributed arrows represent the self-weight uniform load of the main girder. Table 4 lists the model for calculating the internal forces in the vertical direction. The red arrows in the horizontal direction (i.e., X-axis) represents the position of the horizontal inertia force of the trolley, and the black uniformly distributed arrows represents the horizontal inertia force of the main girder. Table 5 lists the calculation

Table 3. Symbols of the main girder force analysis and their physical meaning.

Symbols	Physical meaning	Unit	Symbols	Physical meaning	Unit
S	Crane span	m	b	Trolley wheelbase	m
d	Distance from the position of the small wheel 1 to the centerline of the track of crane truck on the side of the end girder 1	m	D	Track gage of trolley	m
F_G^h	Uniform load in horizontal direction	kN/m	F_G^h	Uniform load in vertical direction	kN/m
P_i^v	Total wheel pressure of trolley wheel i caused by self-weight and lifting weight	kN	P_i^h	Horizontal inertia force of trolley wheel i caused by self-weight and lifting weight	kN

Table 4. Calculation model of the internal force in the vertical direction of the single main girder.

Calculated items		Computational models
Bending moment	Fixed loads	$M_v^u = 0.5F_G^v S d_S - 0.5F_G^v {d_S}^2$
	Mobile loads	$M_v^m = \begin{cases} (P_1^v x_1 + P_2^v x_2)(S-d_S)/S & , x_1 \in [0, d_S - b] \\ (P_1^v x_1 + P_2^v x_2)(S-d_S)/S - P_2^v (x_2 - d_S) & , x_1 \in [d_S - b, d_S] \\ [P_1^v (S - x_1) + P_2^v (S - x_2)] d_S / S & , x_1 \in [d_S, S] \end{cases}$
Shear force	Fixed loads	$F_v^u = F_G^v S / 2 - F_G^v d_S$
	Mobile loads	$F_v^m = \begin{cases} -(P_1^v x_1 + P_1^v x_2)/S & , x_1 \in [0, d_S - b] \\ -(P_1^v x_1 + P_2^v x_2)/S + P_2^v & , x_1 \in [d_S - b, d_S] \\ [P_1^v (S - x_1) + P_2^v (S - x_2)]/S & , x_1 \in [d_S, S] \end{cases}$
Torsional moment	Mobile loads	$T_v^{mi} = P_i^v e$

Note: d_S is the distance from the test section to the centerline of the crane rail on the side of end girder 1 ; x_1 is the distance from trolley wheel 1 to the centerline of the crane rail on the side of end girder 1 ; x_2 is the distance from trolley wheel 2 to the centerline of the crane rail on the side of end girder 1, i.e., $x_2 = x_1 + b$; e is the distance from the bending center of the main girder interface to the centerline of the main web; Unit is mm.

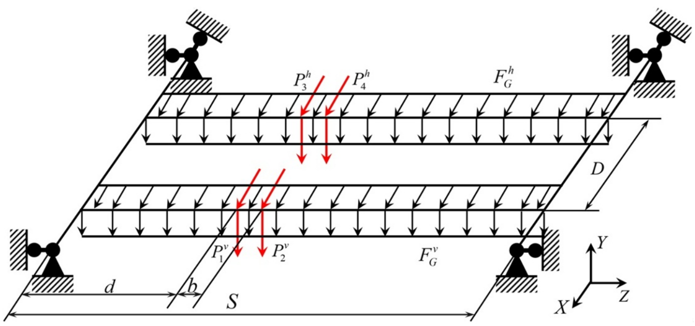

Fig. 4. Sketch of the main girder force of the structural mechanics model of the bridge.

Table 5. Calculation model of the internal force in the horizontal direction of the single main girder.

Calculated items		Computational models
Bending moment	Fixed loads	$M_h^u = 0.5F_G^h S d_S - 0.5F_G^h d_S^{\,2}$
	Mobile loads	$M_h^m = \begin{cases} \left(P_1^h x_1 + P_2^h x_2\right)\left(S - d_S\right) / S & , x_1 \in [0, d_S - b] \\ \left(P_1^h x_1 + P_2^h x_2\right)\left(S - d_S\right) / S - P_2^h (x_2 - d_S) & , x_1 \in [d_S - b, d_S] \\ \left[P_1^h \left(S - x_1\right) + P_2^h \left(S - x_2\right)\right] d_S / S & , x_1 \in [d_S, S] \end{cases}$
Shear force	Fixed loads	$F_h^u = F_G^h S / 2 - F_G^h d_S$
	Mobile loads	$F_h^m = \begin{cases} -\left(P_1^h x_1 + P_2^h x_2\right) / S & , x_1 \in [0, d_S - b] \\ -\left(P_1^h x_1 + P_2^h x_2\right) / S + P_2^h & , x_1 \in [d_S - b, d_S] \\ \left[P_1^h \left(S - x_1\right) + P_2^h \left(S - x_2\right)\right] / S & , x_1 \in [d_S, S] \end{cases}$
Torsional moment	Mobile loads	$T_h^{mi} = P_i^h h$

Note: h is the distance from the top of the trolley track to the neutral layer of the main girder section.

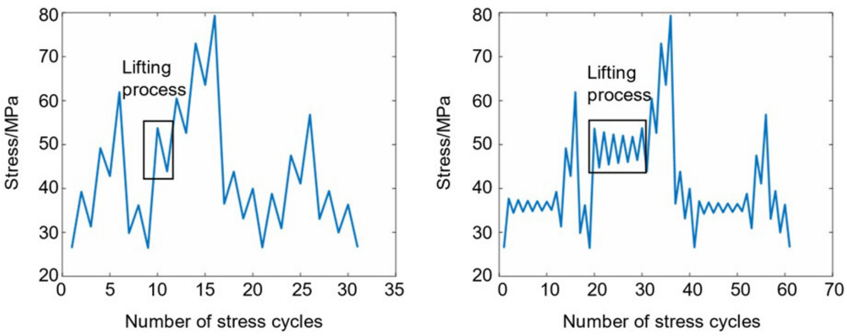

(a) Stress-time history without lifting impact effect

(b) Stress-time history with lifting impact effect

Fig. 5. Stress-time history.

model of internal force in the horizontal direction. As the lifting capacity of the crane changes during service, the concentrated load on the main girder structure also changes.

During crane service, when the lifting capacity, lifting position, and unloading position change, the crane structure is subjected to changing bending moments and shear forces. Since fatigue cracks often occur in the plane of the maximum stress amplitude and expand in the vertical direction of the maximum tensile stress. Therefore, positive and tangential stresses should be transformed into the first principal normal stresses. The calculation model is expressed in Eq. (10).

$$\begin{cases} \sigma_c(t) = M_v(t)/W_x + M_h(t)/W_y \\ \tau_c(t) = F_v(t) S_x / \left[I_x \left(\delta_{\text{web}}^{\text{main}} + \delta_{\text{web}}^{\text{aux}} \right) \right] \\ \qquad + F_h(t) S_y / \left[I_y \left(\delta_{\text{flange}}^{\text{top}} + \delta_{\text{flange}}^{\text{bot}} \right) \right] + T(t) / \left(2 A_0 x_t \right) \\ \sigma_1(t) = 0.5\sigma_c(t) + \sqrt{\left(0.5\sigma_c(t)\right)^2 + \tau_c(t)^2} \end{cases} \quad (10)$$

where $M_v(t)$, $M_h(t)$, $F_v(t)$, $F_h(t)$ are the bending moment course and shear course in the vertical and horizontal directions, respectively; W_x, W_y, S_x, S_y, I_x, I_y are the section modulus, static moment, and moment of inertia in the x- and y-axes, respectively; $\delta_{\text{web}}^{\text{main}}$, $\delta_{\text{web}}^{\text{aux}}$, $\delta_{\text{flange}}^{\text{top}}$, $\delta_{\text{flange}}^{\text{bot}}$ are the thickness of the main and secondary webs and that of the upper and lower flange plates (unit is mm); A_0 is the enclosed area formed by the midline of each plate thickness of the main girder section (unit is mm^2); and x_t is the plate thickness at the test point (unit is mm).

2) Stress variation analysis of the lifting impact

When the crane trolley load is in the initial position, the trolley lifts the cargo from the ground to the designated position. Hence, the lifting process load impact causes structural vibration, leading to dynamic changes in the characteristics of the load on the structure. The quasi-static load law is often used for the equivalent calculation of the dynamic problem of the cargo lifting process, which is used to simulate the load increasing effect of this process by introducing the dynamic load factor [25, 26]. However, in this study, the dynamic modeling method is used to simulate the operation of the crane lifting mechanism. The method can accurately evaluate the impact of the dynamic characteristics generated by the lifting process on the crane structure stress amplitude and the number of stress cycles.

During the lifting phase, the quasi-static load law and dynamics model were used to record the load variations. The calibrated theory of the crane structure was used to obtain the corresponding stress-time history. Fig. 5 shows a crane in a service state in a certain period span of the measurement point stress changes. As shown in Fig. 5(a), there is only one stress cycle during the lifting process when the lifting impact is not considered. However, when the structure is analyzed using a dynamic model of the lifting process (Fig. 5(b)), there is a significant increase in the number of stress cycles in the structure. Therefore, the fatigue remaining life of the crane structure calculation that fully considers the dynamic effects of the lifting process, is crucial for the accurate prediction of the structure's life.

3.3 Rain-flow counting method and stress relief ratio

The rain-flow counting method converts a collection of unordered data into an ordered data matrix and is widely used in crane service information processing. Its main function is to simplify the measured load history into several load cycles and then convert the data into stress mean and amplitude spectra for crane structure hazard points by traversing the entire time history. The resulting data are used for fatigue life estimation and fatigue test load spectrum development. The rain-flow counting method is based on the two-parameter method that considers two variables: stress amplitude and stress mean value.

Since the $da/dN-\Delta K$ curve in the Paris formula in fracture mechanics is based on the stress ratio R = 0 (pulse cycle), the mean and amplitude spectra extracted by the rain-flow counting method should be transformed into the stress variables at R = 0 using Eq. (11).

$$\sigma_0=\frac{2\left(\sigma_a+\dfrac{\sigma_{-1}\sigma_m}{\sigma_b}\right)}{1+\dfrac{\sigma_{-1}}{\sigma_b}} \tag{11}$$

where σ_0, σ_a, σ_m, σ_{-1}, and σ_b are the stress range, stress amplitude, mean of stress, stress amplitude under symmetric cycles, and ultimate strength, respectively.

To facilitate the calculation of fatigue life, the disorganized stress history is addressed using the root-mean-square equivalent stress method, as expressed in Eq. (12). Here, a large amount of data can be combined into an equal amplitude stress variation, and the variable amplitude stress spectrum can be converted into an equal amplitude stress spectrum.

$$\bar{\sigma}=\left(\frac{\sum\sigma_{0i}^{\gamma}n_i}{\sum n_i}\right)^{1/\gamma} \tag{12}$$

where $\bar{\sigma}$ is the equal amplitude stress range (unit is MPa); σ_{0i} is the stress range at all levels (MPa), often eight levels; n_i is the number of cycles that correspond to each level of stress amplitude (unit is number of times); and γ is the damage equivalent parameters. When γ = 2, that is the root-mean-square model.

3.4 Fatigue life evaluation considering the crack closure effect

Structures' fatigue life using fracture mechanics is predicated under the assumption of initial cracking. Therefore, this paper assumes that the crane structure hazard point under study has an initial crack of length a_0. With the existence of initial crack, under high intensity, high-frequency load during a service period will lead to the initial crack size from a_0, gradually expanding to a_1 and leading to fatigue fracture failure. The critical crack size a_1 can be calculated using Eq. (13).

$$a_1=\frac{K_1^2}{\pi Y^2\sigma_{\max}{}^2} \tag{13}$$

where K_1 is the material fracture toughness; Y is the geometric correction factor; and $\sigma_{\max}$ is the maximum cyclic stress. When R = 0, the maximum cyclic stress is equal to the maximum stress variation range.

Based on the isometric stress and critical crack size obtained using root-mean-square equivalence, the fatigue life analysis based on fatigue crack expansion is performed. By integrating the crack expansion formula $da/dN=C_P(U\Delta K)^m$ that considers the crack closure effect, and combining with the average annual number of crane working cycles n_y, the crack expansion time N_y at the dangerous point of the crane structure at the stress cycle characteristic R = 0 is calculated and obtained according to Eq. (14).

$$N_y=\frac{1}{n_y}\begin{cases}\dfrac{1}{C_P\left(UY\bar{\sigma}\sqrt{\pi}\right)^m(0.5m-1)}\left(\dfrac{1}{a_0^{0.5m-1}}-\dfrac{1}{a_1^{0.5m-1}}\right) & (m\neq 2)\\[2ex] \dfrac{1}{C_P\left(UY\bar{\sigma}\sqrt{\pi}\right)^m}\ln\left(\dfrac{a_1}{a_0}\right) & (m=2)\end{cases} \tag{14}$$

where a_0 is the initial crack size (unit is mm); a_1 is the critical crack size (unit is mm); Y is the geometric correction factor; C_P, m is the material parameter; n_y is the number of crane working cycles per year (unit is number of times); N_y is the crane crack expansion time (unit is years); and U is the crack closure effect parameter, which can be determined using Eq. (15) according to Ref. [9]. As the stress ratio R = 0 after the stress-time history treatment using the stress relief ratio method in this study is 3.3, U = 0.69 in this study.

$$\begin{cases}U=\dfrac{1-q}{1-R}\\[1ex] q=0.31\left(1+\dfrac{R}{0.74}\right)\end{cases} \tag{15}$$

Table 6. Basic parameter.

Serial number	Name	Symbols	Value	Unit
1	Self-weight of main girder	m_1	38300	kg
2	Self-weight of trolley	m_2	8850	kg
3	Main girder span	L_1	43	m
4	Trolley wheelbase	l_2	4880	mm
5	Track gage of trolley	L_2	2000	mm
6	Lifting height	l_1	12	m
7	Reel diameter	D	800	mm
8	Rated speed of motor	/	1000	r/min
9	Lifting speed of hook	/	1.25~12.5	m/min
10	Reduction gear ratio	/	31.5	—
11	Motor type	/	YZP250M2-6	—
12	Reducer type	/	ZQ650-3CA	—
13	Brake type	/	YWZ4-300/E80	—

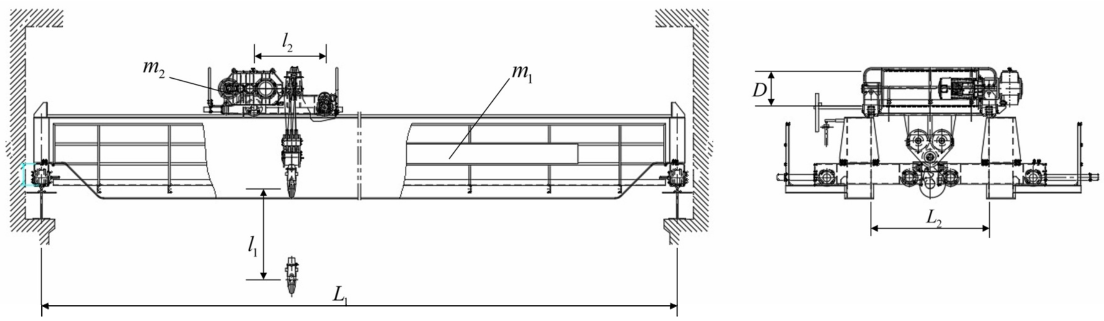

Fig. 6. Simplified model of the entire machine.

where R is the stress ratio and q is the crack tensioning function.

4. Engineering applications

The structure of the bridge crane with a span of 43 m and a lifting capacity of 20 t is the research object. Fig. 6 presents the simplified model of the entire crane structure, and Table 6 shows the relevant parameters presented in the figure.

4.1 Analysis of the lifting impact factor

During the service life of the crane, the dynamic loads have a significant effect on the crack extension effect of the crane structure. When quasi-static load is used to predict the fatigue remaining life of the structure, only the increasing dynamic effects on load amplitude is considered. However, the influence of the number of stress cycles on the structure's life is ignored, inevitably leading to inaccuracy of the evaluation results of the structure's fatigue life. Therefore, the dynamic effects of the lifting process on the remaining life of the crane structure should be clarified when investigating the dynamic characteristics of the lifting process.

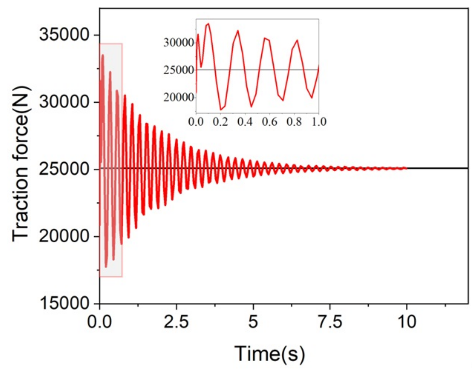

Fig. 7. Wire rope traction force.

In the lifting process of the crane, the parts of the lifting mechanism are in motion before the cargo is lifted off the ground, and the initial parameters and equivalent coefficients of the mechanism are substituted into the corresponding dynamic model to analyze the stress at each point of the main girder. The differential equation of vibration is solved using Simulink, and the change in the traction force of a single wire rope is analyzed (Fig. 7). As shown in Fig. 7, during the lifting of the cargo off the ground, due to the elastic effect of the wire rope and the damping characteristics of the system, the lifting impact causes fluctuations in the traction force and decay with time. As the traction force changes, the stresses at each point on the main girder structure then exhibit the characteristics of dynamic change. According to Eq. (16), the changes in the wire rope traction force are converted to a dynamic lifting load factor, which are multiplied with the lifting weight to obtain the changes of a single cycle load. Finally, the stress-time history of the dynamic lifting process is obtained.

$$\varphi_2 = \frac{nF}{mg} \tag{16}$$

where n is the lifting mechanism of the crane pulley set multiplier, the crane used in this engineering example n = 4; and m is the mass of the lifting cargo.

4.2 Calculation of the fatigue life

The first task of calculating the fatigue life of the crane's metal structures is to analyze stress changes during their operation. Fig. 8 shows the working cycle of the crane in service. During the lifting process, the stress-time history of the lifting impact process is extracted given that the lifting process is part of the working cycle. The figure also shows that the fatigue test point is the welding point between the lower flange plate and sub-web plate in the mid-span section. The point is calculated separately for its fatigue life with and without the lifting shock effect. As shown in Fig. 9, the distribution of the hoisting capacity during the actual 2 months of service is recorded and measured. Because the stress situation at the calculation point of the crane structure is related to the hoisting weight, load position, and other parameters, whether each trolley run passes through the mid-span of the girder should be considered. These data are used as the basis for recording the stress-time history of the crane structure verification point (Fig. 10). Fig. 10(a) shows the stress-time history when dynamic load is calculated using the quasi-static load method, and Fig. 10(b) shows the stress-time history when the lifting impact process is considered. The comparative analysis shows that the number of stress cycles in the crane structure due to the working cycle increases significantly, and the stress amplitude also increases accordingly when the dynamics model is used to analyze the crane's lifting process. Using the fatigue calculation method for cranes based on fracture mechanics, the rain-flow counting method is used to process the stress-time history to obtain the two-parameter stress spectrum (Fig. 11). By analyzing the relevant parameters presented in Fig. 11, the mean values of the stress cycles obtained using the dynamics model are concentrated in the range of 60-80 MPa, and the stress amplitude is small.

The parameters were determined according to the Ref. [24]:

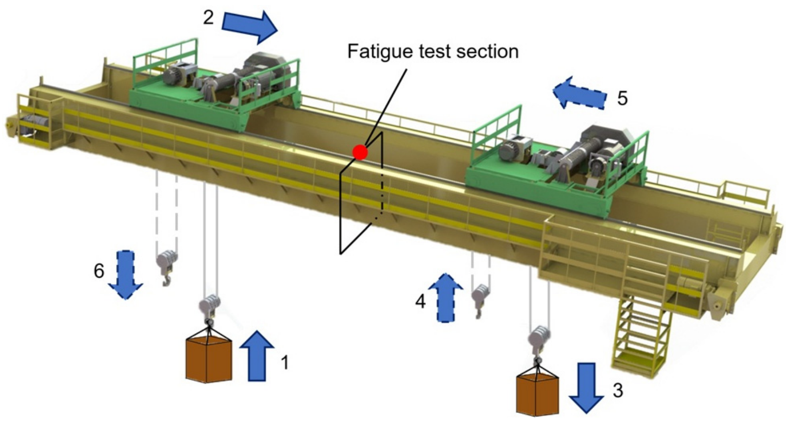

Fig. 8. Crane work cycle (1. for hoist lift, 2. for hoist run, 3. for hoist drop, 4. for no-load lift, 5. for no-load run, 6. for no-load drop).

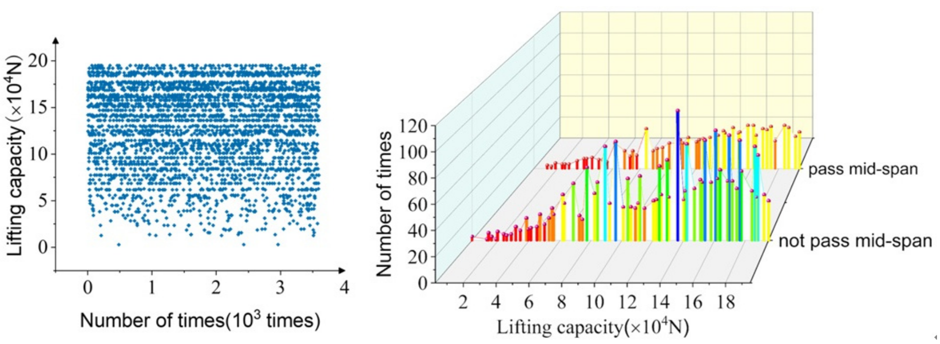

Fig. 9. Lifting capacity - number of lifts.

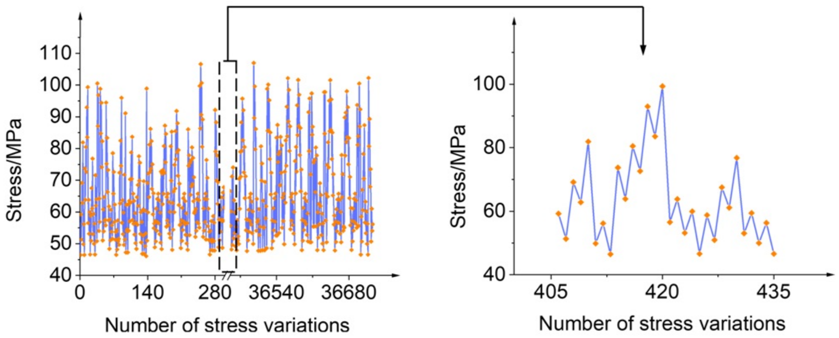

(a) Quasi-static load method

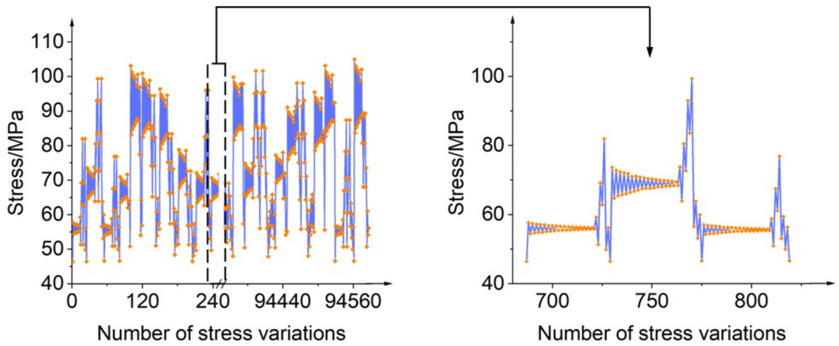

(b) Consider dynamic lifting process

Fig. 10. Stress-time history.

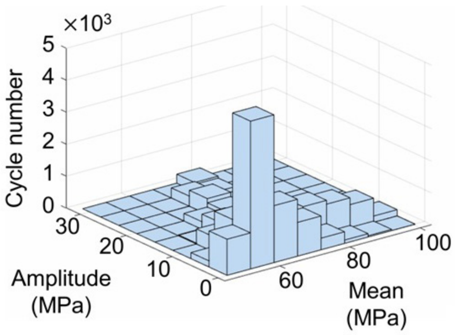

(a) Quasi-static load method

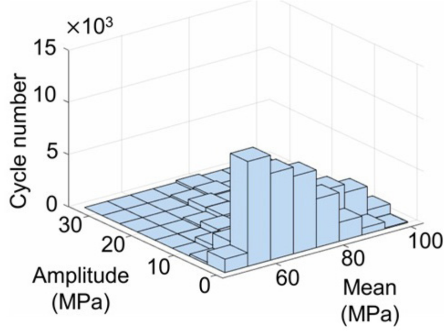

(b) Consider dynamic lifting process

Fig. 11. Two-dimensional, two-parameter stress spectrum.

the initial crack length a_0 = 0.5 mm was obtained; C_P and m were the material parameters, 6.29×10^{-14} and 4.128, respectively; the geometric correction factor Y was 1.2. For the two cases of quasi-static loading method and considering the lifting process, the stress-time histories were processed using the rain-flow counting method, respectively. Their maximum cyclic stresses $\sigma_{\max}$ were obtained as 70.0519 MPa and 73.5001 MPa, respectively. Using Eq. (13), the critical crack sizes a_1 were obtained as 364.87 mm and 331.43 mm. In this study, to compare the crane fatigue life before and after considering the lifting impact process, the actual working conditions of the stress range, for example, a_1 = 200 mm are considered.

Based on the above parameters and using Eq. (14) for fatigue life calculation, the number of years of the fatigue life of the crane metal structure using the conventional quasi-static load method is N_y = 44.53 years, and that using the lifting process dynamics model to calculate the crane metal structure fatigue life is N_y = 41.11 years. This study is based on the life calculation results of the crane lifting mechanism dynamics model, when compared to the conventional calculation method, which is reduced to 7.6 %. This proves that the crane lifting process has a significant impact on the remaining fatigue life of the crane structure, which should be considered in the design of the structure.

4.3 Result analysis and discussion

To determine the fatigue life during crane service and investigate the structural vibration caused by the lifting impact process, a dynamics model was established to match the actual service situation. Load variation caused by the lifting impact process was obtained through the simulation analysis of the dynamics model. The resulting load variation replaces the load obtained by the quasi-static load method into the life cycle of the crane, thus enabling the calculation of the fatigue life of the crane structure considering the lifting impact process. The results indicate that the lifting impact process leads to a significant reduction in the fatigue life of the crane structure. This is mainly because in the lifting impact process, the moment of lifting the cargo off the ground has a surge effect on the value of the crane lifting load, which consequently considerably impacts the displacement and stress at various points of the crane's main girder. As the structural vibration caused by the lifting process gradually smooths out under the effect of damping, the stress in the crane structure constantly changes, and the number of stress cycles increases in each working cycle. This phenomenon results in cumulative accelerating damage to the structure.

5. Conclusion

The dynamic effect of the crane cargo lifting process has a negative impact on the fatigue remaining life of the crane structure. Hence, analysis of the fatigue remaining life of general-purpose bridge crane structures was conducted in this study by combining dynamic modeling methods and fracture mechanics theory. The following are the conclusions of the study:

1) The dynamic characteristics of the lifting process have an impact on the structural stress amplitude and the number of stress cycles. Under the action of the lifting impact, the number of stress cycles of the structure increases, the stress amplitude exhibits a surge during impact, and the amplitude gradually decreases. Therefore, the fatigue load capacity and fatigue residual life of the structure were adversely affects.

2) In the fatigue life prediction of a general-purpose bridge crane structure, the fatigue life of the crane structure is calculated by considering the lifting impact process compared with calculation using the quasi-static load method, which results in a 7.6 % reduction. This result proves that the lifting impact has a remarkable effect on the fatigue life of the crane structure. Based on the results, the proposed method is a good way to complete the dynamic real-time recording of a crane structure, which is useful to obtaining the dynamic response relationship between the lifting impact and the fatigue remaining life of a crane structure. The proposed method can provide an effective technical support for the current crane safety designs.

Acknowledgments

This work was supported by the National Natural Science Foundation of China (No. 52105269 and No. 51805348), and the Excellent Innovation Project for Graduate Students of Taiyuan University of Science and Technology (XCX212067), and the Innovative Project for Graduate Education of Taiyuan University of Science and Technology (SY2022039), China.

References

[1] X. Y. Qi and Z. Xu, Research fatigue life of civil airplane hydraulic tube system based on dynamic stress, *Machine Design and Research*, 34 (3) (2018) 167-170+174.

[2] S. Z. Feng, X. Han and Z. J. Ma, Data-driven algorithm for real-time fatigue life prediction of structures with stochastic parameters, *Computer Methods in Applied Mechanics and Engineering*, 372 (2020) 1-15.

[3] Z. Luo, H. Chen and R. Zheng, A damage gradient model for fatigue life prediction of notched metallic structures under multiaxial random vibrations, *Fatigue and Fracture of Engineering Materials and Structures*, 43 (9) (2020) 2101-2115.

[4] Y. Luo and X. Wu, Fatigue life prediction of box girder of bridge based on equivalent crack approach, *Journal of Mechanical Strength*, 40 (1) (2018) 200-204.

[5] Z. K. Xu, B. Wang and P. Zhang, A fast evaluation method for fatigue strength of maraging steel: The minimum strength principle, *Materials Science and Engineering: A*, 789 (2020) 1-32.

[6] B. W. Wang, X. M. Chen, Y. L. Su and H. B. Sun, Research progress and prospect of fatigue and structural integrity for aeronautical industry in China, *Acta Aeronautica et Astronautica Sinica*, 42 (5) (2021) 1-39.

[7] A. S. Wang, Y. G. Xu and L. H. Xue, Finite element modeling and fatigue life prediction of helicopter composite tail structure under multipoint coordinated loading spectrum, *Composite Structures*, 255 (2021) 1-12.

[8] J. R. Shin, Load spectrum models for offshore crane fatigue analysis, *International Ocean and Polar Engineering Conference*, 31 (4) (2020) 408-486.

[9] Q. Dong, B. He and G. N. Xu, Fatigue life evaluation method for foundry crane metal structure considering load dynamic response and crack closure effect, *Computer Modeling in Engineering and Sciences*, 122 (2) (2020) 525-553.

[10] J. D. Wang, H. Ji and Q. Bian, Stress spectrum and main girder fatigue life estimate for gantry crane, *Engineering Journal of Wuhan University*, 54 (3) (2021) 263-268.

[11] R. M. Nejad and Z. Liu, Effect of periodic overloads and spectrum loading on fatigue life and microstructure in a Grade 900A rail steel, *Theoretical and Applied Fracture Mechanics*, 110 (2020) 1-11.

[12] Y. Y. Chen, Y. K. Liu and Z. W. Wang, Implicit dynamics analysis on the vibration characteristics of crane wheel-rail friction system, *Machinery Design and Manufacture*, 10 (2022) 11-16.

[13] T. Martins, R. Baptista and V. Infante, Numerical study of the Epsilon TB30 aircraft frame, *Engineering Failure Analysis*, 117 (2020) 1-12.

[14] X. G. Qu, X. Wen and X. K. Zhang, Assessing and analysis of the fatigue life of the bridge-type crane based on the damage mechanics, *Journal of Safety and Environment*, 21 (3) (2021) 1012-1016.

[15] N. Lu and C. R. Han, Fatigue life analysis of tower crane

boom based on ADAMS rigid flexible coupling model, *Journal of Mechanical and Electrical Engineering*, 38 (8) (2021) 1003-1009.
[16] J. J. Liu, Y. Ma and S. W. Cao, Fatigue life evaluation on welded joints of tower crane based on equivalent structural stress method, *Journal of Shenyang University of Technology*, 43 (5) (2021) 522-528.
[17] M. Yang, Z. Chang and G. Xu, Analysis on fatigue life of overhead travelling crane girder under impact load for sustainable transport system, *IET Intelligent Transport Systems*, 14 (11) (2020) 1426-1432.
[18] G. Q. Wei, K. Hu and Z. Yu, Simulation of whole fatigue life field of main crane beam considering moving load, *Hoisting and Conveying Machinery* (2021) 47-53.
[19] G. Ávila, E. Palma and R. D. Paula, Crane girder fatigue life determination using SN and LEFM methods, *Engineering Failure Analysis*, 79 (2017) 812-819.
[20] M. Euler and C. Taylor, Fatigue action on crane runway beams, *Journal of Constructional Steel Research*, 181 (2020) 1-15.
[21] P. Rettenmeier, E. Roos and S. Weihe, Fatigue analysis of multiaxially loaded crane runway structures including welding residual stress effects, *International Journal of Fatigue*, 82 (2016) 179-187.
[22] X. Y. Li, X. B. Duan, X. C. Huang and X. Wang, Transient response simulations of telescopic boom of truck cranes, *Journal of Hebei University of Technology*, 46 (3) (2017) 35-38.
[23] Y. S. Xin, Q. Dong and G. N. Xu, Influence of rail joint defects on the running impact coefficient and fatigue residual life of crane, *Journal of Mechanical Engineering*, 56 (14) (2020) 254-264.
[24] Z. Y. Zhao, Study on method of crack diagnosing, controlling and maintaining and its application for mechanical load-carrying structures, *Ph.D. Dissertation*, Wuhan University of Technology (2001) DOI：10.7666/d.Y410917.
[25] National Standards of P. R. C, GB/T3811-2008, *Design Rules for Cranes*, China Standards Press, Beijing (2008) (in Chinese).
[26] ISO, ISO20332:2016, *Crane-Proof of Competence of Steel Structures*, ISO (2016).

Qisong Qi is an Associate Professor and master supervisor at Taiyuan University of Science and Technology. He received his Ph.D. degree from Taiyuan University of Science and Technology. His main research interests include crane modern design theory and design method research, structural optimization design and intelligent optimization algorithm research.